Journal of Bioenergetics and Biomembranes, Vol. 24, No. 1, 1992

Minireview

Toward the Molecular Structure of the Mitochondrial Channel, VDAC

Carmen A. Mannella,[1,2] Michael Forte,[3] and Marco Colombini[4]

Received September 7, 1992

A summary is presented of the most recent information about the structure and mechanism of closure of the mitochondrial channel, VDAC. Considerable information has come from studies involving electron microscopy of two-dimensional crystals and from electrophysiological studies of wild-type channels and site-directed mutants. Available evidence points to a β-barrel as the basic structural model for VDAC. Two models for voltage- or effector- induced closure have been proposed, the first involving removal of strands from the wall of the pore, the second invoking movement of protein domains into the lumen. Experimental strategies to resolve the actual mechanism are presented.

KEY WORDS: Mitochondrial outer membrane; VDAC; membrane channel; voltage gating; electron microscopy; membrane crystals; site-directed mutagenesis.

BACKGROUND

The mitochondrial outer membrane is a physical barrier separating the metabolic processes of the cytoplasm from those of the mitochondrion. The flux of metabolites across this membrane is essential to the processes occurring in both compartments. The only clearly identified protein that mediates this flux is the channel-forming protein called VDAC[5] (Schein *et al.*, 1976; Colombini, 1989; Mannella and Colombini, 1984; Linden *et al.*, 1982a; Freitag *et al.*, 1982). The intent of this review is to summarize the available information about this important mitochondrial component. The most recent data from functional and structural studies are pesented along with models and hypotheses about the molecular mechanisms underlying its very interesting properties.

Functional Characteristics of VDAC

Based on what has been and is being learned about VDAC, it is unlikely that this channel simply converts the outer membrane into a course sieve. When reconstituted into planar phospholipid membranes, VDAC channels are voltage-gated (Schein *et al.*, 1976; Colombini, 1989). At low membrane potentials the channels are open, but they switch to partially closed states in response to elevated voltages (positive or negative) and certain macromolecular modulators (Colombini *et al.*, 1987; Holden and Colombini, 1988). The closed states are less permeable to small ions and possibly impermeable to larger metabolites such as ATP (Benz *et al.*, 1988, 1990; Liu and Colombini, 1991). The open channels favor the flux of anions, displaying a 2 : 1 preference to chloride over potassium, while the closed states are cation selective. The fact that these properties are highly conserved in mitochondria from all eukaryotic king-

[1]Wadsworth Center for Laboratories and Research, New York State Department of Health, Empire State Plaza, P.O. Box 509, Albany, New York 12201-0509.

[2]Department of Biomedical Sciences, School of Public Health, State University of New York at Albany, Albany, New York 12201-0509.

[3]Vollum Institute for Advanced Biomedical Research, Oregon Health Sciences University, Portland, Oregon 97201.

[4]Laboratories of Cell Biology, Department of Zoology, University of Maryland, College Park, Maryland 20742.

[5]Abbreviations: M_{av}, average molecular weight; R_{se}, Stokes-Einstein radius; VDAC, voltage-dependent, anion-selective channel.

0145-479X/92/0200-0007$06.50/0

doms (Colombini, 1989) suggests that VDAC may serve as a site for regulation of mitochondrial function.

The size of VDAC's pore has been estimated by finding the largest nonelectrolyte that passes through the pore (Colombini, 1980a,b; Zalman *et al.*, 1980). (This approach is more reliable than estimating pore size from fluxes of ions, which respond to both steric and electrostatic barriers.) The largest nonelectrolytes that cross VDAC are polyethylene glycol (M_{av} = 3400; R_{se} = 1·9 nm), inulin (M_{av} = 5000; R_{se} = 1.4 nm), and dextran (M_{av} = 6000). A straightforward interpretation of a pore diameter of about 4 nm may be an overestimate because these solute molecules could deform and thus penetrate a smaller opening. In the closed state (Colombini *et al.*, 1987), the channels are not permeable to inulin or polyethylene glycol (M_{av} = 1500; R_{se} = 1·2 nm) but still a bit permeable to gamma cyclodextrin, a rather rigid cyclic molecule (R_{se} = 0.84). Thus the closed state seems to be about 1.8 nm in diameter. These values are in reasonable agreement with values obtained from electron-microscopic observations (see below).

STRUCTURAL INFORMATION FROM ELECTRON MICROSCOPY

The Nature of Information from Electron Microscopy

Considerable information about the structure of VDAC has come from electron microscopic studies of two-dimensional crystals of the channel. While such crystals occur sporadically in outer membrane fractions isolated from *Neurospora crassa* mitochondria (Mannella, 1982), they are induced in large numbers when the same membranes are treated with soluble phospholipase A_2 (Mannella, 1984, 1986). Several different crystalline forms (or polymorphs) of the VDAC protein are observed which have been examined in the transmission electron microscope after various preparative techniques, including:

—*negative staining*, in which the membranes are air-dried in a thin layer of a heavy-metal salt (such as uranyl acetate) or aurothioglucose;

—*freeze-dried/shadowed*, in which unstained membranes are rapidly frozen and dried, and a thin metal coating deposited by evaporation;

—*vitreous-ice embedding (frozen-hydrated)*, in which unstained membranes are fast-frozen in a thin layer of vitreous (noncrystalline) ice at liquid-nitrogen temperature and directly examined in the electron microscope.

Each electron microscopic technique has its own advantages and disadvantages and each provides complementary information about the crystals. The first two, negative staining and metal shadowing, make a cast of the membranes, filling in cavities and outlining surface protrusions. Thus, projection images and computer reconstructions of these specimens primarily relate surface topography. On the other hand, images of unstained, frozen-hydrated membranes are maps of projected density analogous to those obtained by x-ray crystallography. In these images one "sees into" the membrane and so obtains information about its protein, lipid, and water domains in the most native state one can achieve in the electron microscope. A problem with frozen-hydrated specimens is that they are more susceptible to radiation damage than metal-coated specimens. While some protection against the effects of radiation is provided by keeping the specimen at liquid-nitrogen temperature during imaging, procedures must be used that minimize electron dose.

The Usefulness of Membrane Crystals

The availability of planar crystals of the VDAC protein is important for obtaining high-resolution information about its structure. Ordered two-dimensional arrays may be imaged with low electron dose (thereby minimizing beam damage) and the signal extracted from the noisy images of individual repeating units by computer averaging (e.g., Mannella *et al.*, 1986). In this way, atomic- or near-atomic-resolution structures (i.e. 0.5 nm) may eventually be obtained. At present, the best available VDAC crystals are not yet sufficiently large and well-ordered for atomic resolution and so images are limited to the resolution range 1.0–2.0 nm. Even at this resolution, considerable information about VDAC has been gleaned.

How meaningful is structural information obtained from a channel (or any protein) in an artificial crystalline state? Basically, all proteins may occupy a set of low-energy conformational states in solution (or in membranes), and crystal structures represent a subset of these low-energy states. The generally excellent agreement between protein structures solved by x-ray crystallography and structural information from other techniques (spectroscopic, hydrodynamic, etc.) argues that the states observed in crystals are commonly realized ones. In the case of VDAC, crystals are produced by a procedure much milder than those commonly used to crystallize other proteins (particularly membrane proteins). Phospholipase A_2

gradually removes lipid from the membrane bilayer, causing the VDAC proteins to slowly pack closer together and spontaneously order (Mannella, 1986). In fact, as will be discussed below, there is evidence for several different channel conformations in these crystals. The challenge, therefore, is to determine how the different structural states "frozen" in the crystal polymorphs might relate to functional states of the channel.

Basic Structural Parameters of the VDAC Channel

Pore Size; Wall Thickness

Figure 1 is a comparison of computer-averaged electron microscopic images of the most common form of crystalline VDAC embedded in (A) vitreous ice and (B,C) aurothioglucose, a molecule of glucose to which a gold atom is covalently bound (Mannella *et al.*, 1989; Mannella and Guo, 1990). The basic repeating structure in the planar crystal is a group of six close-packed circular features that are white (low density) in the frozen-hydrated crystal and black (high density) in the gold-glucose-embedded specimen. Three-dimensional reconstruction of tilted uranyl-embedded VDAC crystals indicates that the six circular features are the projections of hollow transmembrane cylinders (i.e., pores) aligned normal to the membrane plane (Mannella *et al.*, 1984). The circles are white in Fig. 1A because they are filled with water and they are black in Fig. 1B,C because they contain gold. The large, symmetric openings on either side of the membrane are clearly visible in Fig. 2A,B, which are surface views of the array after freeze-drying and shadowing with Pt (Thomas *et al.*, 1991b).

The diameter of VDAC's lumen may be inferred from images like those of Fig. 1A–C and Fig. 2A,B to be in the range 2.5–3.0 nm, generally consistent with the pore size obtained from functional assays (above). The center-to-center separation of adjacent channels in the array is as small as 4.3 nm in some locations, indicating that the protein wall forming the lumen is very thin (1 nm or less), at least in places. Also, it is clear from the freeze-dried/shadowed images (Fig. 2A,B) as well as from side views and 3-D reconstructions of the membrane arrays in negative stain (not shown) that there is no raised ridge outlining the channel opening. The wall of the lumen seems to be embedded in the membrane and so it is visible only in the projection images of unstained frozen hydrated crystals (Fig. 1A) as a thin, dark (protein) layer separating the water in the lumen from the surrounding low-density lipid. Modeling studies indicate that the protein wall of the lumen is best fitted by a projected hollow cylinder with a diameter (measured at the middle of the annular wall) of $3.8 \pm 0{\cdot}1$ nm (Mannella *et al.*, 1989).

Exposed Protein Domains

While the protein forming the channel wall is primarily embedded in the membrane, there is evidence that other domains of the VDAC protein may be accessible at the membrane surface, in particular the dark lateral "arms" observed at the corners of the unit cell in the frozen-hydrated array (Fig. 1A) and the elevated plateaus on both membrane surfaces in the same region in the shadowed array (Fig. 2A,B). Direct evidence for surface protein domains has been obtained from experiments with site-directed mutants of VDAC (see below) and from protease accessibility studies (DePinto and Palmieri, 1992). It is possible that these exposed domains correspond to regions in VDAC involved in binding proteins, such as hexokinase (Linden *et al.*, 1982b; Fiek *et al.*, 1982; Nakashima *et al.*, 1986) and the VDAC modulator (Holden and Colombini, 1988).

Polypeptide Stoichiometry

The number of 31-kDa polypeptides which form a functional channel was, until recently, a point of contention. While some biochemical and functional evidence suggests that the channel might be a dimer, estimates of crystal-packing of the array components (based on frozen-hydrated density maps and other considerations) indicate that there is not enough space in the membrane arrays for two 31-kDA polypeptides per VDAC lumen (Mannella, 1987). This issue may have been settled by recent electron scattering measurements made on freeze-dried VDAC arrays with the Brookhaven scanning transmission electron microscope (Thomas *et al.*, 1991b). The value obtained for the mass per unit area of the VDAC membrane array ($1.9 \pm 0{\cdot}2$ kDa/nm^2) strongly argues that each channel is formed by a single 31-kDA polypeptide. This conclusion was extended to individual (i.e., noncrystalline) functional channels by the failure to detect hybrid channels in yeast strains which express both wild-type and mutant VDAC genes (Peng *et al.*, 1992). Although nearly equal amounts of wild-type and mutant channels were detected in these strains, no

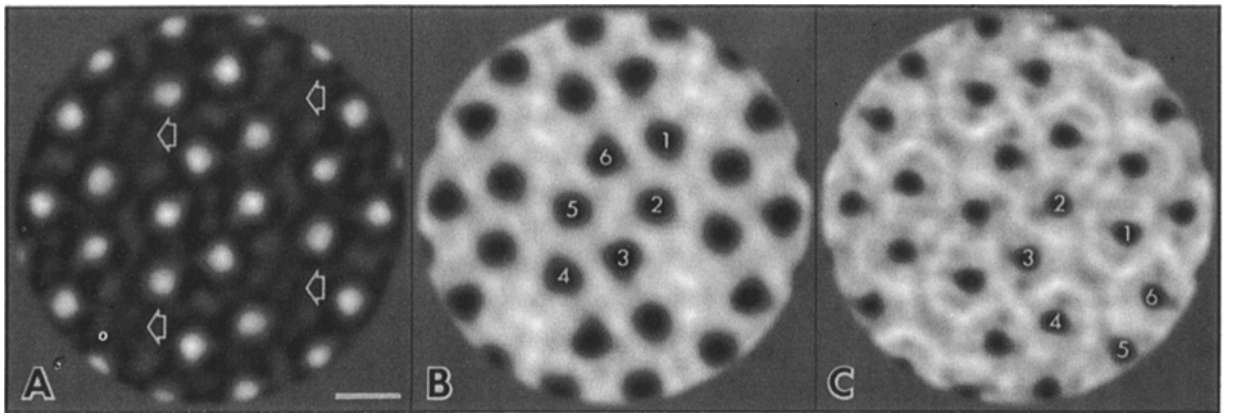

Fig. 1. Computer averages of electron microscopic images of (A) frozen-hydrated and (B,C) aurothioglucose-embedded "oblique" arrays of the VDAC channel. All three arrays were induced in *N. crassa* mitochondrial outer membranes by treatment with phospholipase A_2 (Mannella, 1984). The array in C was exposed to the effector polyanion before embedding. (See text and Mannella and Guo, 1990 for details.) Note the smaller projected diameter of the pores in C than in B. Arrows in A point to the dense "arms" of protein that extend laterally between the channels at the corners of the central unit cell. The six channels inside this unit cell are numbered in B. A different group of six channels, corresponding to a repeat unit suggested by images of freeze-fractured VDAC arrays (Fig. 2C), is numbered in C. Scale bar in A is 5 nm.

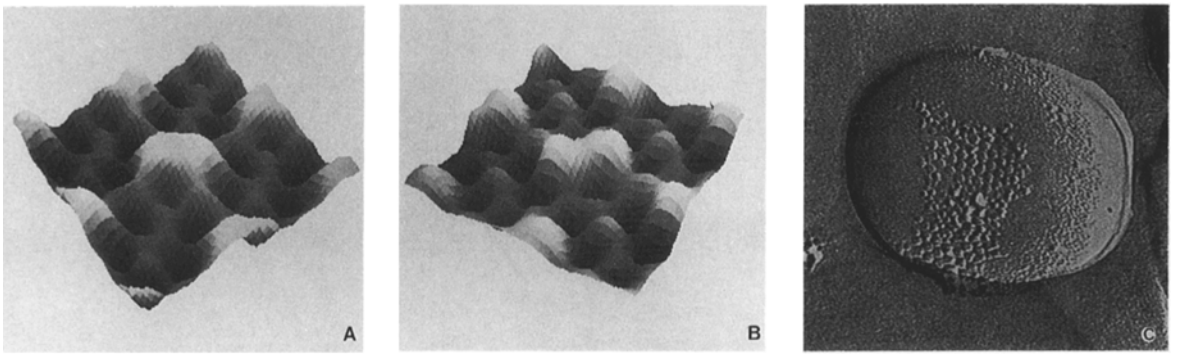

Fig. 2. Surface views of VDAC channels in two-dimensional arrays in outer mitochondrial membranes of *N. crassa*. (A,B) The top and bottom surfaces of induced "oblique" crystals, reconstructed from computer-averaged electron microscopic images of freeze-dried and shadowed specimens. (See Thomas *et al.*, 1991b, for details.) (C) An electron micrograph of a freeze-fractured outer membrane not treated with phospholipase, showing small crystals of VDAC. Each particle is thought to correspond to the 6-channel unit numbered in Fig. 1C. (Figures courtesy of Dr. Lorie Thomas.)

channels with properties expected of a hybrid were found.

Six-Channel Repeating Units

The VDAC arrays in the images of Figs. 1 and 2 represent the most commonly observed lattice type, referred to as "oblique" because of its large lattice angle (109° in Figs. 1 and 2A,B; 117° in Fig. 2C). In parallelogram lattices such as these, any group of six channels with two-fold rotational symmetry may be considered a crystallographic repeating unit. The choice of unit cell in Fig 1B is the convention from the original paper describing these arrays in outer mitochondrial membranes not treated with phospholipase A_2 (Mannella, 1982). It was selected because it defines the most closely packed group of six channels in the array and because this group is invariant in almost all of the observed types of lattice (Mannella *et al.*, 1983; Mannella, 1990). Another possible choice of repeating unit is the "ring" of six channels numbered in Fig. 1C, which surrounds the "arm" or "plateau" region containing (presumably) surface-exposed protein. This repeat unit appears to correlate with the shape of the large hexagonal intramembrane particles observed in small crystalline regions on freeze-fractured outer membranes of *N. crassa* mitochondria untreated with phospholipase (Fig. 2C; Colombini, 1992). The particles are defined by deep grooves which apparently correspond to the location of the channel openings in the monolayer leaflet. At present, no particular functional significance can be attached to any of the possible unit cell choices, since there is no evidence for the VDAC channels occurring in a hexameric grouping outside the crystalline regions.

Polymorphic Forms of the VDAC Crystals: Effector-Induced Changes in the Crystal Lattice

As noted above, there are several different types of VDAC arrays or crystal polymorphs observed with outer membranes from *N. crassa* mitochondria. Lateral transitions can occur in the packing of the channels in the oblique arrays which result in a decrease in the lattice angle to as small as 100° and a reduction in the area of the unit cell by as much as 11% (see Fig. 1 in Mannella *et al.*, 1983 or Fig. 1 in Mannella and Guo, 1990). Since these "contracted" lattices are commonly observed after more prolonged phospholipase A_2 treatment and have greater buoyant density than the "oblique" arrays, they are likely associated with additional loss of lipid (Mannella, 1986). The regions in the VDAC arrays that shrink during lattice contraction are the very regions suspected to contain surface protein (the "arms" of Fig. 1A and the "plateaus" of Fig. 2A,B). Images of frozen-hydrated, contracted lattices of VDAC indicate that the protein arms disappear after contraction (Guo, 1990, 1991), suggesting that protein is displaced from the bilayer in the course of lattice contraction.

It was recently shown that Konig's polyanion, which induces VDAC to close at lower potentials (Colombini *et al.*, 1987), also triggers contraction of the VDAC crystal lattice (Mannella and Guo, 1990). Aluminum, which inhibits VDAC's voltage dependence (Dill *et al.*, 1987), causes the arrays to disorder (Guo, 1991). These effector-induced changes in crystal packing strongly suggest a correlation between the forces controlling long-range order in the crystals and those involved in channel regulation. This in turn suggests that the crystal polymorphs may represent different structural and functional states of the channel.

A STRUCTURAL MODEL FOR VDAC: AN AMPHIPHILIC β-BARREL

Preliminary Considerations and Constraints

As with any protein, the formation of a membrane channel from a polypeptide is driven, in large part, by the free energy difference between the folded structure and the extended chain. Those who study protein folding agree that by far the major driving forces are the hydrophobic interactions. The energy difference between hydrogen bonding with the solvent and intramolecular hydrogen bonding is small. So are the contributions of salt-bridges. The importance of hydrophobic interactions is even more critical for channels (especially channels that form a large aqueous pore) because these are, by their very nature, located at the interface between phases with very different dielectric constants. Thus, the structure that is formed must be "sided," i.e., have a polar surface facing the aqueous environment and an apolar surface facing the lipid membrane.

VDAC's thin wall places further constraints on its structure. Structural and functional evidence (See Polypeptide Stoichiometry) strongly favor the hypothesis that one 30-kDa polypeptide forms one channel. Considering VDAC's large pore radius, the small amount of protein per channel makes it a virtual certainty that the wall of the pore consists of a single

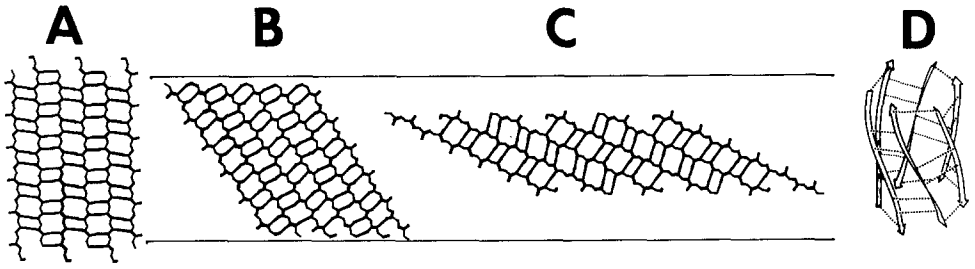

Fig. 3. Geometry of cylindrical β-sheets. (A–C) Backbone structure of antiparallel β-sheets composed of six strands of 12 amino acids each. In A each residue is hydrogen-bonded to a residue on an adjacent β-strand. In B and C, one and two residues, respectively, at both ends of each strand are not hydrogen-bonded. These sheets may be folded into right-cylinders to form antiparallel "β-barrels" normal to the membrane plane, as in D. The horizontal lines in A–C correspond to a membrane thickness of 4 nm. Note that, as the strand tilt increases, the circumference of the corresponding barrel increases and its height decreases. Figure A–C were made by Dr. Stephen Bryant and Michael Bitter (Wadworth Center for Laboratories and Research, Albany, New York) using the Discover and Insight software packages of BioSym Technologies, Inc. installed on a Silicon Graphics computer. Figure D is reproduced from Salemme (1981) with permission of Academic Press.

layer of protein. This expectation is strongly supported by the results with frozen-hydrated samples (See Pore Size; Wall Thickness). Therefore the transmembrane protein strands forming the walls of the pore must be composed of amino acids that alternate between polar and nonpolar residues in a pattern characteristic of the secondary structure of the strand. For an α-helix the pattern should repeat every 3.6 residues while for an extended β-strand it should repeat every other residue. The constraint on the pattern should be limited to the apolar part of the membrane (about 3.5 nm). The pattern should be conserved in different species if the structure is conserved.

For VDAC, indications of an extended β-sheet structure have come from circular dichroism (Mangan and Colombini, unpublished) and from analysis of the primary sequence of the yeast polypeptide. Forte *et al.*, (1987) proposed a model for yeast VDAC in which most of the protein is folded as an amphiphilic cylindrical β-sheet or β-barrel, i.e., a cylinder formed by a single β-sheet whose strands are composed (for the most part) of alternating polar and nonpolar residues. This type of structure is a good candidate for forming aqueous pores through membranes (e.g., Urry *et al.*, 1975), although the actual existence of β-barrel pores has only recently been proven (see below).

Geometry of β-Barrels: Ideal and Actual

Figure 3A–C illustrates the geometrical relationships between strands in ideal antiparallel β-sheets which might be folded uniformly into cylinders (barrels) with long axes normal to the membrane plane. (One such antiparallel β-barrel is shown in Fig. 3D.) Depending on the "ratcheting" of the hydrogen bonds (see legend, Fig. 3), the strands may be untilted or tilted approximately 35 or 60° with respect to the cylinder axis. Of course, as the tilt of the strands increases, the cylinder which they define shortens. For strands of 12 residues as in Fig. 3A–C (the typical length of those detected in VDAC sequences), the cylinder length decreases from about 3.8 to 3.1 to 2.2 nm as the strand tilt increases from 0 to 35 to 60°.

There are numerous examples of β-barrel-containing proteins in nature (e.g., Richardson, 1977). Most are globular, soluble enzymes containing domains of 6–8 parallel β-strands inclined about 35° with respect to the barrel axis (Lasters *et al.*, 1988). Two examples of considerably larger β-barrels are known, the 15-strand, antiparallel barrel of a soluble bacterial chlorophyll-binding protein (Matthews *et al.*, 1979) and the β-barrel forming the lumen of bacterial porins. The latter are 30–50 kDa, pore-forming proteins in the outer envelopes of gram-negative bacteria (Benz, 1985; Nikaido and Vaara, 1985). The structure of the porin from *Rhodobacter capsulata* has been solved at atomic resolution by x-ray crystallography (Weiss *et al.*, 1990) and the atomic structure of *E. coli* PhoE porin is close to being solved by electron crystallography (Jap *et al.*, 1991). The basic structural unit of bacterial porin is a 16-strand antiparallel β-barrel, which is repeated on a three-fold rotation axis to make porin's trimeric functional unit. The β-strands forming the outer wall of the pore are

tilted about 35° with respect to the axis of the β-barrel, while the strands at the interface between adjacent pores in the trimer are tilted about 60°. About 60% of the amino acids in *R. capsulata* porin are used to make the β-barrel; the rest occur in loops and turns connecting the strands of the barrel.

There is no significant sequence homology between VDAC and the bacterial porins (Forte *et al.*, 1987). VDAC's mean lumen diameter (3.8 vs 3.2 nm) and closest interpore spacing (4.3 vs 3.5 nm) are significantly greater than those of the bacterial porins. The electrophysiological properties of the two pores are also very different, including single-channel conductance, ion selectivity, voltage dependence, and interchannel cooperativity. Nonetheless, both porin and VDAC form pores with a high degree of β structure using single copies of relatively small polypeptides (30–32 kDa for VDAC and 30–50 kDa for the porins).

If one assumes that VDAC's lumen is formed by β-strands with a uniform inclination with respect to the cylinder axis, it is a simple matter to predict the number of strands needed to make a cylinder with a C_α-backbone diameter of 3.8 nm (as predicted from density maps of frozen-hydrated specimens; Mannella *et al.*, 1989). Twenty-three strands are required if they are untilted, 19 strands if they are tilted 35°, and 13 strands if their tilt is 60°. In the model proposed for VDAC by Forte *et al.*, (1987) based on the yeast sequence (Mihara and Sato, 1985), most of the polypeptide (over 75% of the residues) is folded into an antiparallel β-barrel of 19 strands. As just noted, such a barrel will have the correct diameter for VDAC if the strands are tilted 35° with respect to the barrel axis. This is the tilt angle commonly observed in known β-barrel domains of soluble proteins and in the region of porin in contact with lipid. Of course, the example provided by bacterial porin suggests that such a model may be an oversimplication, i.e., the strands need not all have the same tilt. It is also possible that additional domains of the protein other than β-strands may be involved in forming the lumen, as will be discussed below.

Identifying the Strands That Form the Wall of the Pore

A search for "sided" β-strands in the available VDAC sequences (human, yeast, and *N. crassa*), by looking for alternating polar/nonpolar patterns in 10-residue stretches of the sequences, reveals a pattern that is rather well conserved (Fig. 4A–C; Blachly-Dyson *et al.*, 1989). The higher the peaks in the β-patterns of Fig. 4, the better the alternating polar/nonpolar pattern. By contrast, applying the same analysis to sequences of other channel-forming proteins of similar size that are thought to form β-barrels yields dramatically different patterns (Fig. 4D–E). Interestingly, long nonpolar stretches of amino acids, characteristic of α-helices in a hydrophobic membrane environment, are not present in VDAC sequences. Focusing on the yeast sequence, one can identify 12 major peaks of sided β structure and a few minor peaks. The first 20 amino acids can form an amphiphilic or sided α-helix (Kleene *et al.*, 1987) and have been implicated as a targeting sequence that participates in directing VDAC to the outer mitochondrial membrane (Mihara and Sato, 1985). Based on this analysis, a model of VDAC consisting of a barrel made up of 1 α-helix and 12 β-strands has been proposed (Fig. 5; Blachly-Dyson *et al.*, 1989). In addition to being defined by amino acid stretches that could form good "sided" structures, most of the proposed strands are delimited by structure breakers: prolines or adjacent charged residues. While the number of strands was not a constraint used to generate the model, as noted above, a barrel composed of 13 transmembrane polypeptide strands would fit the two-dimensional density map of crystalline VDAC, provided the strands are tilted about 60° with respect to the barrel axis.

The model was tested by changing the net charge at specific locations on the molecule and determining the effect of the change on the selectivity of the resulting channels (Blachly-Dyson *et al.*, 1990). Appropriate sites for mutation were selected either in proposed transmembrane strands or in intervening loops. In most cases, the observed results agreed well with the 12-strand-plus-helix model proposed on the basis of the analysis described above. For example, if the conversion of a lysine to glutamate resulted in a reduction in VDAC's anion preference, the strand containing the substitution was considered to be transmembranous. When such an amino acid substitution was introduced in a proposed intervening loop, no change in selectivity provided support for the location of the segment ouside the pore. When selectivity changes were observed they were, by and large, discrete and proportional to the change in charge engineered into the protein. Indeed, the introduction of multiple mutations resulted in a selectivity change

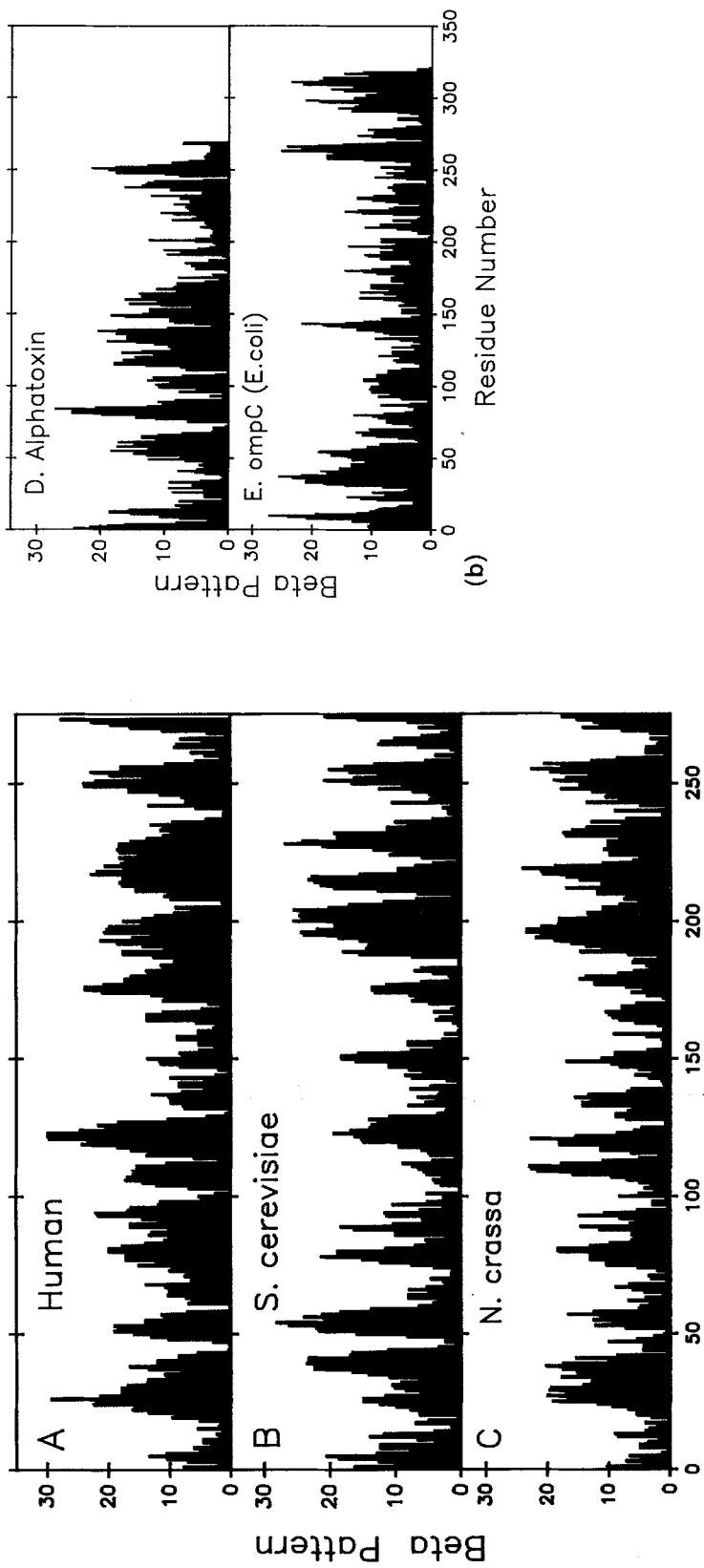

Fig. 4. The tendency of segments of the amino acid sequence of various proteins to form β-strands suitable to line the walls of a water-filled pore. The hydropathy values (Kyte and Doolittle, 1982) of groups of 10 adjacent amino acids were combined as previously described (Blachly-Dyson *et al.*, 1989):

$$\sum_{i=1}^{10} (-1)^{i+1}\, v(i)$$

where $v(i)$ is the hydropathy value of the ith amino acid. The absolute value of each summation was plotted against the number of the first amino acid in the summation. The higher the peak, the better the alternating polar/nonpolar pattern, and the more likely the segment is to form part of the wall of a water-filled pore. (A,B,C) The sequences of VDAC from human (Kayser *et al.*, 1989), yeast (Mihara and Sato, 1985), and *N. crassa* (Kleene *et al.*, 1987), respectively. (D,E) The sequences of α-toxin (Gray and Kehoe, 1984) and OmpC, a "porin" from *E. coli* (Mizuno *et al.*, 1983).

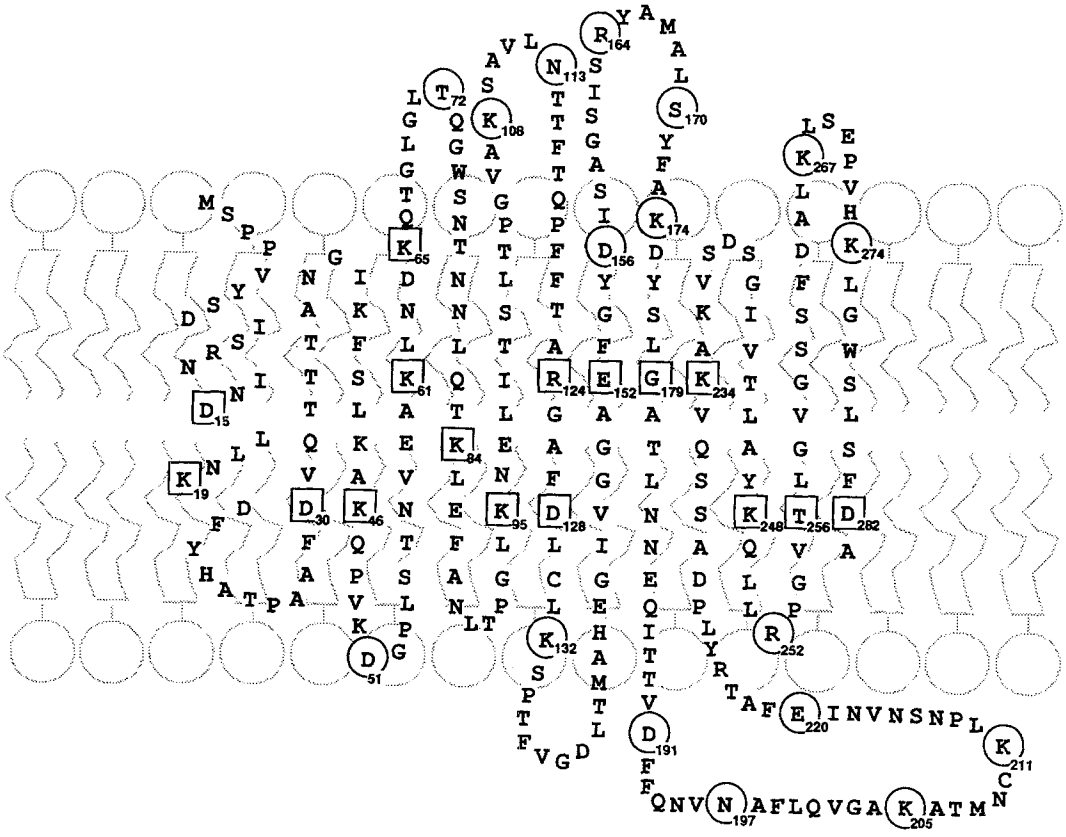

Fig. 5. A 13-strand-barrel model consistent with the "β patterns" for VDAC in Fig. 4 and the results of site-directed mutations. If the α-helix and 12 β-strands were to be tilted by approximately 60° and rolled into a cylinder, they would form a structure consistent with the properties of VDAC's open state. Amino acid substitutions that altered the net charge at a location either shifted the channel's selectivity by a discrete amount (boxed residues) or had no significant effect (circled residues).

that was essentially a linear addition of the effects of the individual mutations.

While the transmembrane location of the α-helix and most of the proposed transmembrane β-strands were confirmed, one proposed β-strand was found not to be transmembranous by the criterion that charge changes in it did not influence the channel's selectivity. In addition, changes in the sequence corresponding to one of the minor peaks in the β-strand pattern of Fig. 4B did influence selectivity, and this region is now designated as the first transmembrane strand next to the α-helix. Although the "sided" nature of this strand is not strong in yeast VDAC, it is very strong (i.e., displays tall peaks in the β-patterns of Figs. 4A,C) in both human and *N. crassa*. Being adjacent to the α-helix, the two threonines which seem to face the lipid bilayer may rather hydrogen-bond with the α-helix. Other weak peaks in the β-strand pattern of yeast VDAC were tested in the same way, especially those corresponding to peaks in the other VDAC sequences, but charge changes in these did not influence channel selectivity.

The N-Terminal α-Helix

The location, with respect to the membrane, of the N-terminal 24-amino-acid segment of VDAC is controversial. In the three known VDAC sequences, this segment is predicted to be able to form an α-helix with a polar face and a nonpolar face. Such a structure could either reside near the membrane surface (i.e., at the interface between the polar headgroups and the nonpolar bilayer core) or be one of the transmembrane strands forming the wall of the aqueous pore. That the latter is the case is strongly indicated by amino acid substitution experiments. Two site-directed mutations in this region clearly alter the selectivity of the channel, as would be expected for an intralumenal location of the residues. Aspartate-to-lysine substitution at

position 15 increases the anion selectivity while a lysine-to-glutamate substitution at position 19 reduces the anion selectivity of the channel (Blachly-Dyson *et al.*, 1990). However, there is evidence that antibodies specific for the N-terminal region of mammalian and fungal VDAC bind both to mitochondria and to crystalline VDAC arrays (DePinto and Palmieri, 1992; Mannella, Stanley, and D'Arcangelis, unpublished results). This suggests that at least part of this region must be accessible to the antibodies at least some of the time. It is possible that a dynamic equilibrium exists that allows the helix to be exposed to the outer surface under certain conditions (See e.g., Proposed Gating Mechanisms). It should also be noted that the mutation work was performed on yeast VDAC and the antibody work on animal and *N. crassa* VDAC. In addition, the former experiments were done on individual channels reconstituted in planar membranes while the later were performed on VDAC in the mitochondrial outer membrane. Thus, the apparent differences in accessibility of the N-terminal segment of the VDAC protein may be related to differences in experimental systems.

Conclusions

Two types of β-barrel are consistent with both the projected density map and primary structure of VDAC: a 19-strand β-barrel with strands tilted about 35° with respect to the barrel axis and a 13-strand cylinder composed of 12 β-strands plus the N-terminal α-helix at a tilt of about 60°. The tilt of the strands in the former model is consistent with that of known β-barrel proteins. Also, this model yields a protein cylinder that spans the full 3–3.5 nm hydrophobic core of the membrane bilayer. However, the most straightforward interpretation of the electrophysiological experiments with site-directed mutants is that there are only 13 lumen-forming protein strands. In this case, only about half of the residues in the VDAC sequence would be involved in forming the walls of the lumen, the rest comprising several long loops that may contribute to the raised surface domains between the pores. As already noted, these domains could act as a binding site for hexokinase and the VDAC modulator and also serve as a mechanism by which adjacent channels interact forming the two-dimensional crystal. The severe tilt, 60°, of the protein strands in the latter model, needed to form a pore with the correct diameter, means that the lumen walls may be as short as 2 nm at some locations. This length is small compared with the membrane's hydrophobic core but may be consistent with the apparent depression of the channel openings in the membrane surface of the freeze-dried/shadowed VDAC array (Fig. 2A,B). The gramicidin dimer, whose overall length is 2.6 nm, forms long-lived channels in phospholipid membranes. In thicker, solvent-containing membranes, open times are decreased, presumably due to distortion of the lipid bilayer (Finkelstein and Andersen, 1981).

MECHANISMS FOR CLOSURE

Characteristics of the Closed States of VDAC

The VDAC channel can exist in various conformational states. This is clear not only from the existence of crystalline polymorphs (See Structural Information from Electron Microscopy) but also from functional studies. The latter have demonstrated the existence of a clearly defined high-conducting state, referred to as the open state, and a multiplicity of low-conducting, closed states (Colombini, 1989). While there are clearly multiple open states, their properties are much less varied than those of the closed states. The membrane potential is a major factor (but not the only factor) determining occupancy of these states, i.e., VDAC is voltage-gated. The open state is much preferred at low or zero membrane potential. At higher potentials (generally above 20 mV) channels close. There appears to be a set of closed states for positive potentials and another for negative potentials.

In order for the different states to be observed and for the channel to function as a voltage-gated channel, the energy difference between the different states must be small. In VDAC the energy difference between these states is 10 k j/mol (Bowen *et al.*, 1985), about 1/3 of a hydrogen bond. However, there is overwhelming evidence that the structural changes are large. Upon channel closure: (1) the effective pore diameter drops from about 3 to about 1.8 nm, based on measurements of polymer permeability (Colombini *et al.*, 1987); (2) the volume of the pore decreases by about 30 nm^3, as inferred from effects of osmotic pressure on VDAC closure (Zimmerberg and Parsegian, 1986); and (3) the ionic selectivity reverses from preferring anions to preferring cations, with a change in permeability ratio of a factor of 10 for KCl (Colombini, 1980b; Zhang and Colombini, 1990). In addition, there is evidence that lysine residues associated with channel gating move through the membrane

based on succinic anhydride accessibility experiments (Doring and Colombini, 1985) and preliminary studies on channels altered by site-directed mutagenesis (Thomas *et al.*, 1991a). Binding sites for aluminum hydroxide also seem to be translocated through the membrane (Zhang and Colombini, 1990).

Proposed Gating Mechanisms

The molecular nature of the conformational changes that take place when VDAC channels open and close has yet to be resolved. In order to understand how these conformational changes occur, it is critical to define the exact nature of the voltage sensor and the way it is coupled to the aqueous conduction pathway as defined by changes in conductance and selectivity. The clues that have been obtained are worth discussing because, for this channel, the degrees of freedom have been severely limited by experimental observations. Any proposed mechanism must account for all experimental observations including the energetics of the voltage-gating process.

Evidence from Ion Selectivity Changes in Site-Directed Mutants

One approach to defining VDAC's gating mechanism is to compare the electrophysiological characteristics of the open and closed states of site-directed mutants. This is possible because the closed state is still permeable to KCl, although it may be impermeable to larger molecules such as adenine nucleotides. Therefore, selectivity changes can still be measured in the closed state. The results show that some strands that contain residues that effect ion selectivity in the open state no longer do so in the closed state (Peng *et al.*, 1991). The simplest interpretation is that these residues lie in protein segments that form part of the wall in the open state but are pulled out of the channel upon closure, resulting in a smaller pore diameter and pore volume (consistent with experimental observations). Another consequence of this interpretation is a radical change in the net charge on the wall of the pore, consistent with the large change in selectivity of the channel in the closed state. Furthermore, the movement of strands out of the pore could result in the net movement of charge through the membrane potential, a requirement for voltage gating. This model predicts that the strands that move out of the pore must be part of the voltage sensor and that charge changes in these regions must influence the voltage dependence of the channels in a very predictable way. Experiments to test these predictions are under way and so far this expectation has been confirmed at a number of locations in the channel.

Evidence from Electron Microscopy

Another approach to defining the changes in VDAC associated with closure is to study the effects of conditions known to alter VDAC's functional state on the structure of membrane crystals of the channel. As noted in Structural Information from Electron Microscopy, the polyanion that increases VDAC's voltage dependence also induces contraction of the crystal lattice (Mannella and Guo, 1990). This structural transition involves the displacement from the membrane surface of the protein "arms" detected in projection images of frozen-hydrated oblique arrays, allowing the channels to pack closer together (Guo, 1990, 1991). In addition to this change in packing geometry, the polyanion also causes the mean projected diameter of VDAC's pore to decrease, both in oblique and contracted arrays (Fig. 1B,C; Mannella and Guo, 1990). The decrease observed in pore size (from about 2.5 to 1.7 nm) is close to that expected for the change from VDAC's open to closed states on the basis of functional studies (See Mechanisms for Closure).

The fact that VDAC's pore size can decrease significantly without altering the packing of the channels in the oblique array suggests that closure (at least in its initial phases) may not involve a significant change in the outer diameter of the channel wall. In order to explain this observation, a mechanism for closure has been proposed (Mannella, 1990) that involves movement of one or more protein domains into the lumen. In the open state, these movable parts of the VDAC protein are the lateral arms observed in the oblique array (Fig. 1A). Displacement of these protein arms from the membrane surface (e.g., by an amphiphilic or lipophilic substance, such as the polyanionic effector) is a necessary but not sufficient condition for lattice contraction (i.e., lipid must also be removed). Once the arms are freed from the membrane surface, they may interact with the rest of the VDAC protein. Entry of the arms into the lumen would amount to partial closure and might also trigger further conformational changes leading to more fully closed states. Altered selectivity of the channel could arise either from screening of fixed charges in the lumen by the inward-moving parts of the protein or from more complex changes in the lumen structure induced by this movement.

There is preliminary evidence that the arms observed in the frozen-hydrated images and implicated in this closure mechanism are composed, at least in part, of the N-terminal domain of the VDAC protein. Fab fragments derived from antibodies raised against a peptide corresponding to residues 1–20 in the *N. crassa* VDAC sequence bind to the region in the oblique arrays containing the protein arms (Guo and Mannella, unpublished results). While the α-helix has virtually no net charge or dipole moment (when the side chains are considered) and thus cannot alone account for the voltage dependence, some other (unspecified) outside domain may contain sufficient charge to account for the voltage dependence of the process. On the surface, this closure mechanism is inconsistent with the selectivity changes induced by site-directed mutations, since it puts the N-terminal α-helix outside the pore in the open state. However, more complex structures may account for the data.

Reconciling the Two Gating Models

The two models presented above for the gating mechanism of VDAC are diametrically opposed but readily experimentally distinguishable. The first explains closure in terms of the removal of "staves" of the β-barrel that forms the wall of VDAC's lumen. The second mechanism proposes that closure is initiated by movement of part of the protein into the interior of the lumen. Both mechanisms are consistent with a large volume change in the pore associated with closure, as well as with altered ion selectivity. Ultimately, determining the molecular details of closure will require improved understanding of the basic structure of this channel and of its functional and biochemical topology in different functional states. Systematic investigations of the effects of charge changes along VDAC's sequence on its voltage dependence will be essential to identifying the sensor region(s) in the molecule. Likewise, combining high-resolution three-dimensional electron microscopy with antibody probes of specific segments of the VDAC polypeptide should define which parts of the protein are accessible in different functional states of the channel.

FUTURE PROSPECTS

Despite its apparently simple structure, VDAC has a rather broad repertoire of behavior. It has two voltage-gating processes, one at positive and the other at negative potentials. VDAC also responds to macromolecules including a variety of polyanions and a mitochondrial protein, the VDAC modulator. There is much evidence indicating that VDAC is the site of hexokinase binding to mitochondria. There is also evidence that microtubules may bind to VDAC via a MAP protein (Linden *et al.*, 1989). The structural features involved in these effects need to be identified and the processes understood.

Sterols appear to be tightly bound to VDAC (Pfaller *et al.*, 1985), but how these fit into VDAC's structure is unclear. They may provide rigidity, restrict possible conformations, fill cavities between the protein and phospholipid environment, or have some other role. This is an essentially unexplored area.

More recently, there have been reports that VDAC-like molecules are located on the surface of cell membranes (Thinnes, 1992). If confirmed, this finding raises numerous questions: Are these proteins channels and are they identical to VDAC in mitochondria? Is there a VDAC gene family? How might VDAC molecules be targeted to different membranes? Finally, one might wonder how common extended β-structures are in channels in general. It is interesting to note that, despite the early attention paid to transmembrane α-helices in the sodium and potassium channels, recent results strongly indicate that the ion pathways in these channels are formed by β-strands (e.g., Guy and Conti, 1990). Only time will tell to what extent the different classes of channels share common structural motifs and mechanisms.

ACKNOWLEDGMENTS

One of the authors (C.A.M.) wishes to thank Dr. Stephen Bryant for many helpful discussion in the course of writing this review. The research summarized in this paper is supported by National Science Foundation grant DMB-8916315 to C.A.M., National Institutes of Health grant GM 35759 to M.F., and Office of Naval Research grant N00014–90–J–1024 to M.C.

REFERENCES

Benz, R. (1985). *CRC Crit. Rev. Biochem.* **19,** 145–190.
Benz, R., Wojtczak, L., Bosch, W., and Brdiczka, D. (1988). *FEBS Lett.* **231,** 75–80.
Benz, R., Kottke, M., and Brdiczka, D. (1990). *Biochim. Biophys. Acta* **1022,** 311–318.
Blachly-Dyson, E., Peng, S. Z., Colombini, M., and Forte, M. (1989). *J. Bioenerg. Biomembr.* **21,** 471–483.

Blachly-Dyson, E., Peng, S. Z., Colombini, M., and Forte, M. (1990). *Science* **247,** 1233–1236.
Bowen, K. A., Tam, K., and Colombini, M. (1985). *J. Membr. Biol.* **86,** 51–59.
Colombini, M. (1980a). *J. Membr. Biol.* **53,** 79–84.
Colombini, M. (1980b). *Ann. N.Y. Acad. Sci.* **341,** 552–563.
Colombini, M. (1989). *J. Membr. Biol.* **111,** 103–111.
Colombini, M. (1992). In *Membrane Electrochemistry* (Blank, M., Vodyanoy, I., and Hong, F., eds.), American Chemical Society, Washington, DC, in press.
Colombini, M., Yeung, C. L., Tung, J., and König, T. (1987). *Biochim. Biophys. Acta* **905,** 279–286.
Depinto, V., and Palmieri, F. (1992). *J. Bioenerg. Biomembr.* **24,** 21–26.
Dill, E. T., Holden, M. J., and Colombini, M. (1987). *J. Membr. Biol.* **99,** 187–196.
Doring, C., and Colombini, M. (1985). *J. Membr. Biol.* **83,** 87–94.
Fiek, C., Benz, R., Roos, N., and Brdiczka, D. (1982). *Biochim. Biophys. Acta* **688,** 429–440.
Finkelstein, A., and Anderson, O. S. (1981). *J. Membr. Biol.* **59,** 155–171.
Forte, M., Guy, H. R., and Mannella, C. A. (1987). *J. Bioenerg. Biomembr.* **19,** 341–350.
Freitag, H., Neupert, W., and Benz, R. (1982). *Eur. J. Biochem.* **123,** 629–639.
Guo, X. W. (1990). In*Proceedings of the XIIth International Congress for Electron Microscopy* (Peachey, L. D., and Williams, D. B., eds.), San Francisco Press, San Francisco, pp. 100–101.
Guo, X. W. (1991). *Electron Microscopic Studies of 2D Membrane Crystals of Mitochondrial Channel, VDAC,* PhD Thesis, State University of New York at Albany.
Gray, G. S., and Kehoe, M. (1984). *Infect. Immun.* **46,** 615–618.
Guy, H. R., and Conti, F. (1990). *Trends Neurosci.* **13,** 201–206.
Holden, M. J., and Colombini, M. (1988). *FEBS Lett.* **241,** 105–109.
Jap, B. K., Walian, P. J., and Gehring, K. (1991). *Nature (London)* **350,** 167–169.
Kayser, H., Kratzin, H. D., Thinnes, F. P., Gotz, H., Schmidt, W. E., Eckart, K., and Hilschmann, N. (1989). *Biol. Chem. Hoppe–Seyler* **370,** 1265–1278.
Kleene, R., Pfanner, N., Pfaller, R., Link, T., Sebald, W., Neupert, W., and Tropschug, M. (1987). *EMBO J.* **6,** 2627–2633.
Kyte, J., and Doolittle, R. F. (1982). *J. Mol. Biol.* **157,** 105–132.
Lasters, I., Wodak, S. J., Alard, P., and van Cutsem, E. (1988). *Proc. Natl. Acad. Sci. USA* **85,** 3338–3342.
Linden, M., Gellerfors, P., and Nelson, B. D. (1982a). *Biochem. J.* **208,** 77–82.
Linden M., Gellerfors, P., and Nelson, B. D. (1982b). *FEBS Lett.* **141,** 189–192.
Linden, M., Nelson, B. D., and Leterrier, J.-F. (1989). *Biochem. J.* **261,** 167–173.
Liu, M. Y., and Colombini, M. (1991). *Biochim. Biophys. Acta,* in press.
Mannella, C. A. (1982). *J. Cell Biol.* **94,** 680–687.
Mannella, C. A. (1984). *Science* **224,** 165–166.
Mannella, C. A. (1986). In *Methods in Enzymology* (Fleischer, S., and Fleischer, B., eds.), Academic Press, London, pp. 595–610.
Mannella, C. A. (1987). *J. Bioenerg. Biomembr.* **19,** 329–340.
Mannella, C. A. (1990). *Experientia* **46,** 137–145.
Mannella, C. A. and Colombini, M. (1984). *Biochim. Biophys. Acta* **774,** 206–214.
Mannella, C. A., and Guo, X. W. (1990). *Biophys. J.* **57,** 23–31.
Mannella, C. A., Colombini, M., and Frank, J. (1983). *Proc. Natl. Acad. Sci. USA* **80,** 2243–2247.
Mannella, C. A., Radermacher, M., and Frank, J. (1984). In *Proceedings of the 42nd Annual Meeting of the Electron Microscopy Society of America* (Bailey, G. W., eds.), San Francisco Press, San Francisco, pp. 644–645.
Mannella, C. A., Ribeiro, A., and Frank, J. (1986). *Biophys. J.* **49,** 307–318.
Mannella, C. A., Guo, X. W., and Cognon, B. (1989). *FEBS Lett.* **253,** 231–234.
Matthews, B. W., Fenna, R. E., Bolognesi, M. C., Schmid, M. F., and Olson, J. M. (1979). *J. Mol. Biol.* **131,** 259–285.
Mihara, K., and Sato, R. (1985). *EMBO J.* **4,** 769–774.
Mizuno, T., Chou, M.-Y., and Inouye, M. (1983). *J. Biol. Chem.* **258,** 6932–6940.
Nakashima, R. A., Mangan, P. S., Colombini, M., and Pedersen, P. L. (1986). *Biochemistry* **25,** 1015–1021.
Nikaido, H., and Vaara, M. (1985). *Microbiol. Rev.* **49,** 1–32.
Peng, S., Blachly–Dyson, E., Colombini, M., and Forte, M. (1991). *Biophys. J.* **59,** 215a.
Peng, S., Blachly-Dyson, E., Colombini, M., and Forte, M. (1992). *J. Bioenerg. Biomembr.* **24,** 27–32.
Pfaller, R., Freitag, H., Harmey, M. A., Benz, R., and Neupert, W. (1985). *J. Biol. Chem.* **260,** 8188–8193.
Richardson, J. S. (1977). *Nature (London)* **268,** 495–500.
Salemme, F. R. (1981). *J. Mol. Biol.* **146,** 143–156.
Schein, S. J., Colombini, M., and Finkelstein, A. (1976). *J. Membr. Biol.* **30,** 99–120.
Thinnes, F. P. (1992). *J. Bioenerg. Biomembr.* **24,** 71–76.
Thomas, L., Blachly-Dyson, E., Colombini, M., and Forte, M. (1991a). *Biophys. J.* **59,** 215a.
Thomas, L., Kocsis, E., Colombini, M., Erbe, E., Trus, B. L. and Steven, A. C. (1991b). *J. Struct. Biol.* **106,** 161–171.
Urry, D. W., Long, M. M., Jacobs, M., and Harris, R. D. (1975). *Ann. N.Y. Acad. Sci.* **264,** 203–220.
Weiss, M. S., Wacker, T., Weckesser, J., Welte, W., and Schulz, G. E. (1990). *FEBS Lett.* **267,** 268–272.
Zalman, L. S., Nikaido, H., and Kagawa, Y. (1980). *J. Biol. Chem.* **255,** 1771–1774.
Zhang, D.-W., and Colombini, M. (1990). *Biochim. Biophys. Acta* **1025,** 127–134.
Zimmerberg, J., and Parsegian, V. A. (1986). *Nature (London)* **323,** 36–39.